Acta Pharmacologica Sinica

www.nature.com/aps

ARTICLE

Atranorin inhibits NLRP3 inflammasome activation by targeting ASC and protects NLRP3 inflammasome-driven diseases

Hao-yu Wang[1,2], Xi Lin[3], Guan-gen Huang[2,3], Rong Zhou[2], Shu-yue Lei[1,2], Jing Ren[2,3], Kai-rong Zhang[2,4], Chun-lan Feng[2], Yan-wei Wu[2,5] and Wei Tang[1,2,3]

Aberrant NLRP3 activation has been implicated in the pathogenesis of numerous inflammation-associated diseases. However, no small molecular inhibitor that directly targets NLRP3 inflammasome has been approved so far. In this study, we show that Atranorin ($C_{19}H_{18}O_8$), the secondary metabolites of lichen family, effectively prevents NLRP3 inflammasome activation in macrophages and dendritic cells. Mechanistically, Atranorin inhibits NLRP3 activation induced cytokine secretion and cell pyroptosis through binding to ASC protein directly and therefore restraining ASC oligomerization. The pharmacological effect of Atranorin is evaluated in NLRP3 inflammasome-driven disease models. Atranorin lowers serum IL-1β and IL-18 levels in LPS induced mice acute inflammation model. Also, Atranorin protects against MSU crystal induced mice gouty arthritis model and lowers ankle IL-1β level. Moreover, Atranorin ameliorates intestinal inflammation and epithelial barrier dysfunction in DSS induced mice ulcerative colitis and inhibits NLRP3 inflammasome activation in colon. Altogether, our study identifies Atranorin as a novel NLRP3 inhibitor that targets ASC protein and highlights the potential therapeutic effects of Atranorin in NLRP3 inflammasome-driven diseases including acute inflammation, gouty arthritis and ulcerative colitis.

Keywords: Atranorin; NLRP3; inflammasome; ASC; acute inflammation; gouty arthritis; colitis

Acta Pharmacologica Sinica (2023) 44:1687–1700; https://doi.org/10.1038/s41401-023-01054-1

INTRODUCTION

NOD-, LRR- and pyrin domain-containing protein 3 (NLRP3) is an intracellular sensor that monitors diverse risk factors including pathogen associated molecular patterns (PAMPs) and damage associated molecular patterns (DAMPs) [1]. The activation of NLRP3 inflammasome needs double signals: the priming signal (Signal 1), which is mediated by nuclear factor kappa-B (NF-κB) activation, and the activation signal (Signal 2), which is stimulated by extracellular ligands like adenosine 5′-triphosphate (ATP), Nigericin or Monosodium Urate (MSU) crystal. Upon activation, NLRP3 recruits the adapter molecule apoptosis-associated speck-like protein containing CARD (ASC) and subsequently the effector molecule Pro Caspase-1 to form a large protein complex called NLRP3 inflammasome. Afterward, Pro Caspase-1 self-cleaves and leads to the secretion of IL-1β and IL-18 and pyroptosis.

Being an important part of innate immunity, the activation of NLRP3 inflammasome helps resist pathogen infection and stress damage, whereas the uncontrolled activation would cause the amplification of inflammatory effects and organ damage. The abnormal activation of NLRP3 inflammasome is closely related to the occurrence and development of systemic and multi-organ diseases like acute inflammation [2], gouty arthritis [3] and ulcerative colitis (UC) [4]. Thus, targeting the aberrant activation of NLRP3 inflammasome is applicable for treating these inflammatory diseases [5].

So far, the FDA has not approved any compound that directly targets the NLRP3 inflammasome. Most of the existing intervention strategies target the upstream signals or downstream effector factors rather than NLRP3 inflammasome complex itself [6, 7]. For example, inhibiting priming, which is mediated by NF-κB pathway activation, would produce many off-target effects or even exacerbate NLRP3 inflammasome dependent inflammation since NF-κB pathway has a broad-spectrum impact on innate immunity and adaptive response [8–10]. On the other hand, targeting the downstream effector factors like IL-1β with neutralizing antibody might increase the risk of infection [11, 12]. Hence, there is still urgent need for searching novel inhibitors that directly targeting NLRP3 inflammasome.

Lichens are the symbiotic complex that consists of a fungus and autotrophic photosynthetic species and can grow in diverse and extreme environmental conditions [13]. Atranorin ($C_{19}H_{18}O_8$) is among the secondary metabolites of lichen family with the depside structure (Fig. 1a). The anti-inflammatory activities of Atranorin has been reported, including inhibiting nitric oxide (NO) production [14], inhibiting Leukotriene B4 (LTB4) biosynthesis [15], inhibiting Cyclooxygenase-1 (COX-1) activity [16] and alleviating

[1]University of Chinese Academy of Sciences, Beijing 100049, China; [2]Laboratory of Anti-inflammation and Immunopharmacology, Shanghai Institute of Materia Medica, Chinese Academy of Sciences, Shanghai 201203, China; [3]School of Chinese Materia Medica, Nanjing University of Chinese Medicine, Nanjing 210023, China; [4]School of Pharmaceutical Science, Nanchang University, Nanchang 330006, China and [5]School of Medicine, Shanghai University, Shanghai 200444, China
Correspondence: Yan-wei Wu (wuyanwei@shu.edu.cn) or Wei Tang (tangwei@simm.ac.cn)

Received: 7 November 2022 Accepted: 9 January 2023
Published online: 24 March 2023

carrageenan induced paw edema [17]. At the same time, the acute toxicity assay and the subchronic toxicity assay carried on rats confirm the safety of Atranorin in vivo [17]. However, mechanism study on how Atranorin exerts its anti-inflammatory activity is lacking. Also, the potential application of Atranorin on disease models has not been sufficiently studied.

In this article, we would study the action of Atranorin on NLRP3 inflammasome and attempt to uncover the potential mechanism. We would also test the pharmacologic effect of Atranorin on NLRP3 driven disease models, including Lipopolysaccharide (LPS) induced acute inflammation, MSU crystal induced gouty arthritis and Dextran Sulfate Sodium (DSS) induced UC, so as to explore the clinical applications.

MATERIALS AND METHODS

Reagents and antibodies

Atranorin was kindly provided by Wei-min Zhao (PhD). Iscove's Modified Dulbecco's Medium (IMDM) and Dulbecco's Modified Eagle's Medium (DMEM) were purchased from Gibco (Grand Island NY, USA). Fetal bovine serum (FBS) was purchased from Hyclone (Logan, UT, USA). LPS, ATP, MSU, pronase, FITC-CM-Dextran (average mol wt 4,000), collagenase IV and dispase were purchased from Sigma Aldrich (St. Louis, MO, USA). Val-BoroPro (VbP) was purchased from Aladdin (Shanghai, China). Poly (dA: dT) was purchased from Invivogen (Carlsbad, CA, USA). Recombinant Murine M-CSF, Recombinant Murine IL-4 and Recombinant Murine GM-CSF were purchased from Peprotech (London, UK). DSS (molecular weight 36–50 kDa) was purchased from MP Biomedicals (Irvine, CA, USA). Cell Counting Kit-8 (CCK-8) was purchased from Dojindo (Kumamoto, Japan). ELISA kit for mouse IL-1β, Pierce BCA Protein Assay Kit, AF594 cross-adsorbed secondary antibody were purchased from Thermo Fisher Scientific (Waltham, MA, USA). ELISA kits for mouse TNF-α, IL-6, IL-18 were purchased from eBioscience (San Diego, CA, USA). LDH kit, SDS lysis buffer and NP-40 lysis buffer were purchased from Beyotime (Shanghai, China). Lipofectamine™ 2000 Transfection Reagent (Lipo2000) was purchased from Invitrogen (Waltham, MA, USA). BCA protein assay kit, proteinase and phosphatase inhibitor were purchased from Thermo Scientific (Pittsburgh, PA, USA). Fecal occult blood test kit was purchased from Nanjing Jiancheng Bioengineering Institute (Nanjing, China). RNA simple total RNA kit was purchased from Tiangen (Beijing, China). Hifair™ II 1st Strand cDNA Synthesis SuperMix and Hifair™ qPCR SYBR Green Master Mix were purchased from Yeasen (Shanghai, China). Rabbit anti-mouse NLRP3 (15101S), rabbit anti-mouse ASC (67824S), rabbit anti-mouse Caspase-1 (89332S), rabbit anti-mouse IL-1β (31202S) and rabbit anti-mouse E-cadherin (3195S), and HRP-conjugated anti-α Tubulin (9099S) were purchased from Cell Signaling Technology (Danvers, MA, USA). Rabbit anti-mouse GSDMD (ab209845) was purchased from Abcam (Cambridge, MA, USA). HRP-conjugated anti-GAPDH (KC-5G5) was purchased from Kangcheng (Shanghai, China). HRP-conjugated goat anti-rabbit IgG (1706515) was purchased from Bio-Rad (Richmond, CA, USA).

Cell cultures and in vitro activation of NLRP3 inflammasome

For the differentiation of bone marrow-derived macrophages (BMDM), bone marrow from the tibia and femur bones of C57BL/6 mice was stimulated with Recombinant Murine M-CSF (10 ng/ml) in sterile IMDM supplemented with 10% FBS, 1% penicillin/streptomycin at 37 °C with humidified 5% CO_2 for 7 d. On day 4, the supernatants were removed and replaced with fresh Medium supplemented with stimulators. For the differentiation of bone marrow-derived dendritic cells (BMDC), bone marrow was stimulated with mouse IL-4 and Recombinant Murine M-CSF in sterile RPMI-1640 supplemented with 10% FBS, 1% penicillin/streptomycin at 37 °C with humidified 5% CO_2 for 7 d. On d 3 and d 5, the supernatants were removed and replaced with fresh Medium supplemented with stimulators. After 7 d, BMDM and BMDC were washed with cold PBS, suspended and seeded at the required density for all experiments. The purity of macrophages ($CD11b^+$, $F4/80^+$) and dendritic cells ($CD11b^+$, $CD11c^+$) was consistently >98%.

BMDM or BMDC or RAW264.7 cells were seeded at 4×10^5 cells /ml in 12-well plates. For the activation of NLRP3 inflammasome, cells were primed with LPS (10 ng/ml) for 3 h. Then the medium was removed and replaced with serum-free medium containing Atranorin (100 μM, 50 μM and 25 μM) for 30 min. Cells were subsequently stimulated with the different inflammasome activators for indicated time: ATP (5 mM) for 1 h, Nigericin (10 μM) for 1 h or MSU crystal (300 ng/ml) for 5 h. For the activation non-canonical NLRP3 inflammasome, BMDM were primed with Pam_3CSK_4 (400 ng/ml) for 3 h. Then the medium was removed and replaced with serum-free medium containing Atranorin (100 μM, 50 μM and 25 μM) for 30 min. Cells were subsequently transfected with LPS (1.5 μg/ml) in Lipo2000 for 16 h. For the activation of AIM2 inflammasome, BMDM were primed with LPS (10 ng/ml) for 3 h. Then the medium was removed and replaced with serum-free medium containing Atranorin (100 μM, 50 μM and 25 μM) for 30 min. Cells were subsequently transfected with Poly (dA: dT) (1 μg/ml) in Lipo2000 for 5 h. For the activation of NLRP1B inflammasome, RAW264.7 cells were stimulated with Val-boroPro (2 μM) for 24 h in the presence or absence of Atranorin (100 μM, 50 μM and 25 μM). To study the influence of Atranorin on the priming stage of NLRP3 inflammasome activation, BMDM were primed with LPS (10 ng/ml) in the presence or absence of Atranorin (100 μM, 50 μM and 25 μM) for 3 h. After washing for 3 times, cells were stimulated with ATP (5 mM) or Nigericin (10 μM) for 1 h. Supernatants were collected for ELISA and LDH analysis. Cells were collected for Western blot, RT-PCR or immunofluorescence assay.

CCK-8 assay

BMDM (4×10^4 cells) were cultured in 96-well plates with 200 μl of IMDM supplemented with 10% FBS, 1% penicillin/streptomycin at 37 °C with humidified 5% CO_2. After adhesion, Cells were treated with or without indicated concentrations of Atranorin for 24 h. Subsequently, a total of 20 μl CCK-8 was added to each well. After 2 h incubation, the absorbance value at 450 nm (570 nm calibration) was measured by a microplate reader (Molecular Devices, Sunnyvale, CA, USA) and the cell viability was calculated.

Enzyme-linked immunosorbent assay (ELISA)

Cytokines in cell culture supernatants, serum, tissue explant culture supernatants and tissue homogenates were determined by ELISA kit according to the manufacturer's instructions. The absorbance value at 450 nm (650 nm calibration) was measured by a microplate reader (Molecular Devices, Sunnyvale, CA, USA). Tissues from mice were homogenized with PBS and centrifuged, supernatants were taken for measurement. The concentration of total protein was determined by BCA protein assay kit. The cytokine levels in tissue homogenates were expressed as ng/mg protein and others were expressed as pg/ml or ng/ml.

Western blot

Cells and tissues were lysed with SDS lysis buffer containing proteinase and phosphatase inhibitor. Protein concentration was determined by BCA protein assay Kit. Equal amounts of proteins (10–60 μg) were separated by 10%/12.5% SDS-PAGE and transferred to nitrocellulose membranes. After blocking with 5% BSA, the precut membranes were incubated overnight at 4 °C with primary antibodies. After washing with TBS with Tween-20 (TBST), HRP-conjugated anti-rabbit IgG or HRP-conjugated monoclonal mouse

anti-GAPDH or HRP-conjugated monoclonal mouse anti-α tubulin were added at room temperature for 1 h. Signals were detected with Super Signa West Femto Maximum Sensitivity Substrate (Thermo) under ChemiDoc™ MP Imaging System (Bio-Rad).

LDH detection
BMDC (4×10^5 cells) were cultured in 12-well plates with 1 ml of IMDM supplemented with 10% FBS, 1% penicillin/streptomycin at 37 °C with humidified 5% CO_2. Cells were treated with or without indicated concentrations of Atranorin for 24 h. Then LDH level in supernatants was detected according to the manufacturer's instruction to indicate cell viability. After in vitro activation of inflammasome, LDH level in supernatants was detected according to the manufacturer's instruction to indicate pyroptosis. The absorbance value at 490 nm (650 nm calibration) was measured by a microplate reader (Molecular Devices, Sunnyvale, CA, USA).

Reconstitution of NLRP3 inflammasome in HEK293T cells
This assay was carried out according to a previously described protocol [18]. Briefly, HEK293T cells were transfected with plasmids encoding murine NLRP3 inflammasome components (HA-ASC (20 ng, Addgene, 41553), HA-NEK7 (200 ng, Addgene, 75142), FLAG-Pro caspase-1 (100 ng, Addgene, 75128), FLAG-NLRP3 (200 ng, Addgene, 75127), FLAG-Pro IL-1β (200 ng, Addgene, 75131)) using Lipo2000. Six hours after transfection, medium was replaced with DMEM containing FBS (10%) and penicillin–streptomycin (1%). After 24 h, Atranorin was added to incubate for 0.5 h. Then, Nigericin (10 mM) was added to cells in order to activate the inflammasome. Supernatants were collected 45 min later for ELISA analysis.

RNA extraction and quantitative real-time polymerase chain reaction (RT-qPCR)
Total RNA was isolated from BMDM cells using RNA simple total RNA kit (Tiangen). Then cDNA was derived from 10 μg total RNA by Hifair™ II 1st Strand cDNA Synthesis SuperMix. Real-time PCR was performed on reverse transcription products with specific primers and Hifair™ qPCR SYBR Green Master Mix. Primer sequences were listed in Table S1.

ASC oligomerization assay
BMDM (4×10^6 cells) were seeded in 75 cm^2 dish. After in vitro activation of NLRP3 inflammasome, cells were collected for ASC complex isolation according to a previously described protocol [19]. Briefly, 500 μl of ice-cold buffer (20 mM HEPES-KOH, pH 7.5, 150 mM KCl, 1% NP-40, 0.1 mM PMSF, proteinase and phosphatase inhibitor) was added to cells. Fifty microliters lysates were separated for the detection of uncross-linked ASC and the residues were centrifuged at $330 \times g$ for 10 min at 4 °C. Then the pellets were washed twice in ice-cold PBS and incubated with 2 mM disuccinimydyl suberate (dissolved in 500 μl of PBS) at room temperature for 30 min with rotation. Afterward, the cross-linked pellets were centrifuged at $330 \times g$ for 10 min at 4 °C and resuspended in 30 μl of SDS-PAGE Loading buffer. Samples were boiled for 5 min at 100 °C and analyzed by Western blot.

Immunofluorescence
For the detection of ASC speck, BMDM on coverslips were treated according to our in vitro activation of NLRP3 inflammasome protocol and then fixed with fixing solution (Beyotime, China) for 15 min at room temperature. After blocking for 1 h with the blocking buffer (Beyotime, China), BMDM were incubated with rabbit anti-ASC antibody overnight at 4 °C. The FITC-conjugated anti-rabbit secondary antibody (Proteintech) was added and incubated for 1 h at room temperature. The nuclei were counterstained with DAPI. The images were captured using Leica TCS SPS CFSMP microscope (Wetzlar, Germany).

For the detection of NLRP3 activation in colon macrophages and dendritic cells, paraffin-embedded colon slices were dewaxed with xylene and hydrated through graded ethanol to water, followed by unmasking epitope in 0.01 M citrate buffer solution. The colon tissue samples were then blocked with 5% BSA and stained with anti-Caspase-1 p20, FITC-conjugated F4/80 (eBioscience)/FITC-conjugated CD11c (eBioscience) overnight at 4 °C. Unconjugated fluoresceins were further conjugated with AF594 cross-adsorbed secondary antibody and the nuclei were counterstained with DAPI (Abcam). Images were subsequently captured using Olympus VS200 Slide scanner.

Cellular thermal shift assay (CETSA)
CETSA was performed according to a previously reported protocol [20]. Briefly, BMDM were pre-incubated with Atranorin (100 μM) for 2 h. Cells were harvested with cell scraper and resuspended in PBS containing protease inhibitor. Then the cell suspensions were divided into nine aliquots and heated at various temperature via PCR instrument, respectively. The heat-treated cell suspensions were freezed and thawed twice in liquid nitrogen. The cell lysis was centrifuged at $10{,}000 \times g$ for 20 min at 4 °C to separate the soluble fraction from precipitates. The supernatants were collected for Western blot analysis.

Drug affinity responsive target stability (DARTS)
DARTS was performed according to a previously reported protocol [21]. Briefly, BMDM were lysed with NP-40 lysis buffer containing protease inhibitor on ice. The lysates were centrifuged at $10{,}000 \times g$ for 10 min at 4 °C. Protein concentration was measured with a Pierce BCA Protein Assay Kit (Thermo) and was adjusted to 2 mg/ml. Lysates were incubated with Atranorin (400 or 200 or 100 or 50 or 25 μM) for 1 h at room temperature. Then, pronase (20 ng of enzyme per μg of protein, Sigma) was added to the lysates (20 μg of protein lysate per reaction) and incubated for 20 min at room temperature. The reaction was stopped by the addition of 1× SDS loading buffer. Then, the samples were boiled at 95 °C for 10 min followed by Western blot analysis.

Animals
Male and Female C57BL/6 mice (6–8 weeks, 18–20 g), and female BALB/c mice (6–8 weeks, 18–20 g) were obtained from Shanghai Lingchang Biotechnology Co. Ltd (Certificate No. 2013–0018, China). Mice were maintained at the specific pathogen-free (SPF) animal facilities of Shanghai Institute of Materia Medica with 12 h of light/12 h of dark cycle, 22 ± 1 °C and 55% ± 5% of relative humidity, and were given free access to food and water. All experiments performed in this article were in accordance with the Guidelines for the Care and Use of Laboratory Animals published by the United States National Institutes of Health and were also approved by the Institutional Animal Care and Use Committee (IACUC) at Shanghai Institute of Materia Medica.

LPS induced acute inflammation model
Female BALB/c mice were randomly divided into four groups (normal, vehicle, Atranorin 100 mg/kg and Atranorin 50 mg/kg) with five mice per group. Atranorin treated groups were administered orally with 100 or 50 mg/kg Atranorin (dissolved in 0.2% Tween 80) and vehicle group was administered with the solvent 0.2% Tween 80. After 1 h, the vehicle group and Atranorin treated groups were injected intraperitoneally with 5 mg/kg LPS (dissolved in PBS) while the normal group was injected with PBS. After 2 h, mice were euthanatized, and serum IL-1β, IL-18, TNF-α and IL-6 levels were measured by ELISA.

MSU crystal induced gouty arthritis model
Male C57BL/6 mice were randomly divided into five groups (normal, vehicle, Atranorin 100 mg/kg and Atranorin 50 mg/kg)

with five mice per group. Atranorin treated groups were administered orally with 100 or 50 mg/kg Atranorin (dissolved in 0.2% Tween 80) and vehicle group was administered with the solvent 0.2% Tween 80. After 1 h, the vehicle group and Atranorin treated groups were injected intra-articularly with 200 μg MSU crystal (dissolved in PBS) while the normal group was injected with PBS. Ankle swelling was measured at different time points using a precision caliper. After 24 h, mice were euthanatized, and the ankle joints were collected for explant culture. The IL-1β level in explant culture supernatants was measured by ELISA.

DSS induced ulcerative colitis model

Female C57BL/6 mice were randomly divided into four groups (normal, vehicle, Atranorin 100 mg/kg and Atranorin 50 mg/kg) with nine mice per group. Atranorin treated groups were administered orally with 100 or 50 mg/kg Atranorin (dissolved in 0.2% Tween 80) and vehicle group was administered with the solvent 0.2% Tween 80 daily for 7 d. UC was induced by administration of DSS (3% in sterile water) for 5 d and then sterile water for another 2 d. The disease activity indexes (DAI) including body weight loss, stool consistency and fecal blood were recorded daily. The criteria of the calculated scores of DAI is defined as follows: body weight loss (0, none; 1, 1%–5%; 2, 6%–10%; 3, 11%–20%; 4, >20%); stool consistency (0, normal; 1, soft but still formed; 2, soft; 3, very soft and wet; 4, watery diarrhea); fecal blood (0, negative hemoccult; 1, weakly positive hemoccult; 2, positive hemoccult; 3, blood traces in stool visible; 4, gross rectal bleeding). Mice were euthanatized on d 7, then colon and spleen were collected for the following analysis. For colon tissue explant culture, colon was washed with cold PBS to remove fecal contents and cut into equal fragments (1 cm long). Then the fragments were cultured for 24 h in 0.8 ml RPMI-1640 supplemented with 10% FBS, 1% penicillin/streptomycin at 37 °C with humidified 5% CO_2. Supernatants of colon explant culture were collected for ELISA analysis.

Colon histology

For the evaluation of colon damage, colon tissues were fixed in 4% paraformaldehyde at room temperature and H&E staining was performed by Servicebio Company (Wuhan, China). Histological evaluation of H&E-stained colonic sections is graded as follows: 0, no signs of inflammation; 1, low leukocyte infiltration; 2, moderate leukocyte; 3, high leukocyte infiltration, moderate fibrosis, high vascular density, thickening of the colon wall, moderate goblet cell loss, and focal loss of crypts; 4, transmural infiltrations, massive loss of goblet cell, extensive fibrosis, and diffuse loss of crypts.

FITC-CM-dextran intestinal permeability assay

Intestinal permeability was assessed by oral gavage of nonmetabolizable macromolecule FITC-CM-dextran. Mice were administered 200 μl FITC-CM-dextran (600 mg/kg) by oral gavage 4 h before sacrifice. Then serum was obtained for the measurement of FITC–dextran by fluorescence plate reader (Ex: 488 nm, Em: 525 nm). For observing permeable fluorescence signal directly, mice were exposed to the IVIS Spectrum CT system (Perkin Elemer) and the fluorescent retentions were measured at 480 nm excitation and 520 nm.

Statistical analysis

All experiments were repeated at least three times and data were presented as mean ± SEM. Statistical differences were analyzed by GraphPad Prism 8.0 software (La Jolla, CA, USA) using one-way analysis of variance (ANOVA). $P < 0.05$ was considered statistically significant, with increasing levels of confidence displayed as $^{*}P < 0.05$; $^{**}P < 0.01$.

RESULTS

Atranorin inhibits the activation of NLRP3 inflammasome in BMDM

To investigate the effect of Atranorin (Fig. 1a) on NLRP3 inflammasome activation, we first tested the cytotoxicity of Atranorin on mouse BMDM and the non-cytotoxic concentrations (25 μM, 50 μM and 100 μM) were chosen in the following experiments (Fig. 1b). We primed BMDM with LPS followed by Atranorin treatment. Afterward, ATP/Nigericin/MSU crystal was added to activate NLRP3 inflammation. We observed that upon NLRP3 inflammasome activation, BMDM lost pseudopod and turned into round and swelled morphology while Atranorin could prevent this process (Fig. 1c). Atranorin also inhibited the secretion of IL-1β and IL-18 levels in BMDM culture supernatants, whose release is the hallmark of NLRP3 inflammation activation (Fig. 1d). IL-1β is cleaved by Caspase-1. Correspondingly, Atranorin dose-dependently decreased the amount of Caspase-1 p20/p10 (the autoprocessed fragment of Caspase-1) and IL-1β p17 (the active form of IL-1β) in culture supernatants, but did not inhibit the expression of NLRP3, ASC, Pro Caspase-1 (the precursor of Caspase-1) and IL-1β in cell lysates (Fig. 1e). Pyroptosis is another consequence of NLRP3 inflammasome activation besides inflammatory cytokines release. Atranorin decreased pyroptosis induced LDH release (Fig. 1f) and pyroptosis executor cleaved GSDMD protein level in BMDM (Fig. 1g). Apart from canonical NLRP3 inflammasome activation, cytosolic LPS could be sensed by Caspase-4/5/11 to induce non-canonical NLRP3 inflammasome activation. We primed BMDM with Pam_3CSK_4 and then transfected with LPS to induce non-canonical NLRP3 inflammasome activation. Atranorin also inhibited non-canonical NLRP3 inflammasome activation induced IL-1β release (Fig. 1h). All the above results indicate that Atranorin inhibits NLRP3 inflammasome activation in BMDM.

Atranorin inhibits the activation of NLRP3 inflammasome in BMDC and NLRP3 inflammasome-reconstituted HEK293T cells

Besides macrophages, NLRP3 is also widely expressed in dendritic cells [22]. We then examined the effect of Atranorin in BMDC to further verify the inhibition effect of Atranorin on NLRP3 inflammasome. Correspondingly, at non-toxic concentrations (Fig. 2a), Atranorin inhibited IL-1β and IL-18 release (Fig. 2b) and caspase-1 cleavage (Fig. 2c), as well as pyroptosis induced LDH release in BMDC (Fig. 2d). Moreover, we reconstituted NLRP3 inflammasome in HEK293T cells by transfecting plasmids encoding the components of NLRP3 inflammasome complex including NEK7, NLRP3, ASC, Pro caspase-1, Pro IL-1β into HEK293T cells. Atranorin also inhibited IL-1β secretion stimulated by Nigericin in NLRP3 inflammasome-reconstituted HEK293T cells (Fig. 2e). All these results confirm the inhibitive effect of Atranorin on NLRP3 inflammasome.

Atranorin inhibits the assembly of NLRP3 inflammasome complex through binding to ASC

Next, we investigated the mechanism through which Atranorin suppresses NLRP3 inflammasome activation. We first determined if Atranorin influences the priming stage of NLRP3 inflammasome activation. We incubated Atranorin at priming stage and washed before the activation stage. Atranorin did not affect the transcript of *Nlrp3* and *Il-1β* (Fig. S1a), which is medicated by LPS induced NF-κB activation. Also, Atranorin did not inhibit LDH release when applied at the priming stage (Fig. S1b). These results indicate that Atranorin acts on the activation stage rather than the priming stage to inhibit NLRP3 inflammasome activation. During NLRP3 inflammasome activation, ASC would self-associate into a helical fibrillary assembly, resulting in formation of ASC oligomer and ASC speck, which provide molecular platform for the activation of Pro Caspase-1 autocatalytic cleavage [23]. Atranorin treatment significantly attenuated the

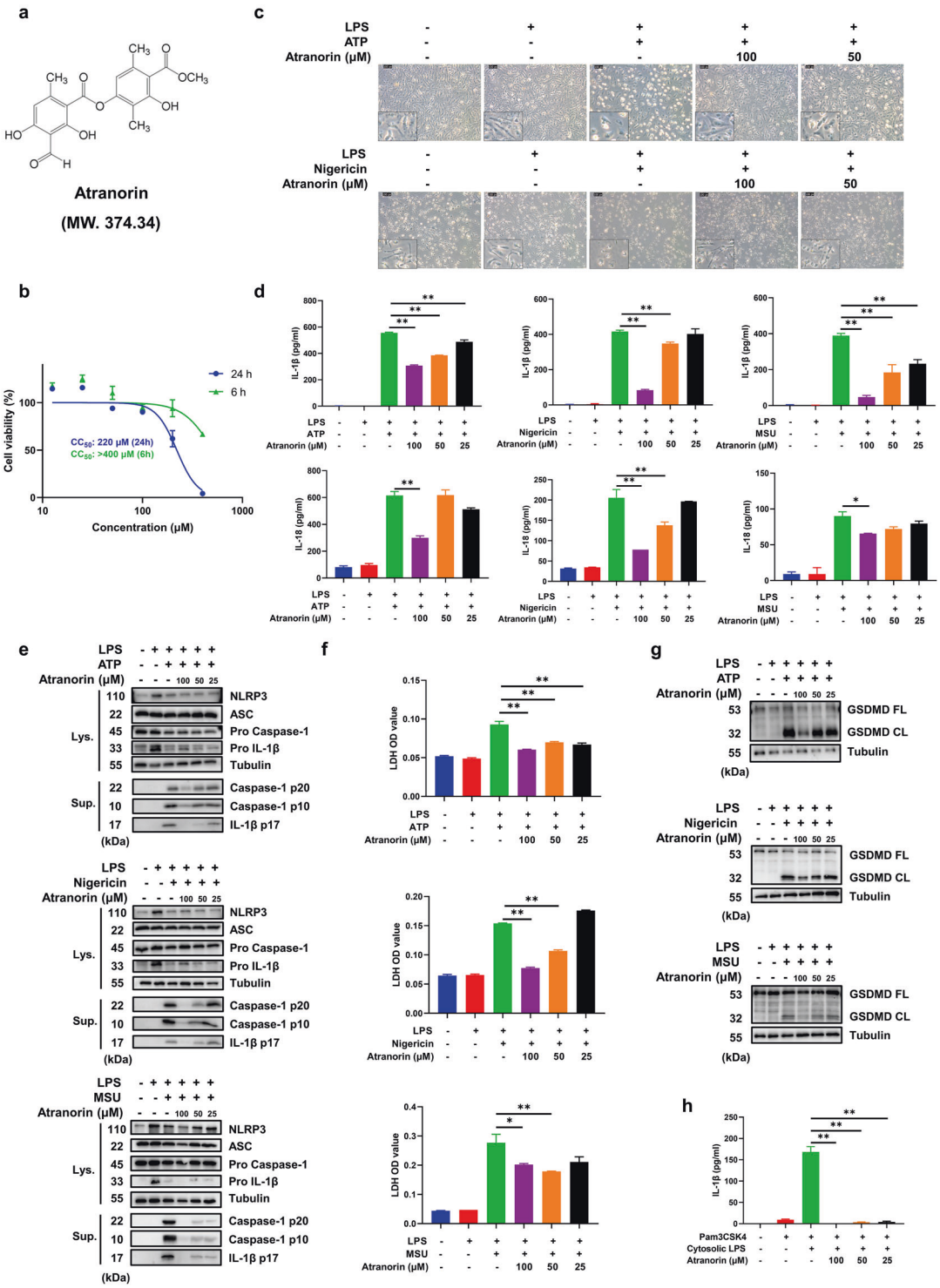

Fig. 1 Atranorin inhibits the activation of NLRP3 inflammasome in BMDM. a The structure of Atranorin. **b** The cytotoxicity of Atranorin on BMDM was detected by CCK-8 kit. **c**–**g** BMDM were primed with LPS and then stimulated with ATP/Nigericin/MSU crystal in the presence or absence of different doses of Atranorin. Morphology of BMDM (**c**) was observed under phase contrast microscope. IL-1β and IL-18 levels in culture supernatants (**d**) were measured by ELISA. The protein levels of NLRP3, ASC, Pro Caspase-1 and Pro IL-1β in cell lysates and cleaved Caspase-1 and cleaved IL-1β in resin concentrated supernatants (**e**) were detected by Western blot. The LDH level in cell culture supernatants (**f**) was measured by LDH kit. GSDMD full length and cleaved GSDMD in cell lysates (**g**) were measured by Western blot. **h** BMDM were primed with Pam_3CSK_4 and then transfected with LPS in the presence or absence of different doses of Atranorin. IL-1β level in culture supernatants was measured by ELISA. Data were shown as Mean ± SEM from triplicate measurements. $^*P < 0.05$, $^{**}P < 0.01$ compared as indicated.

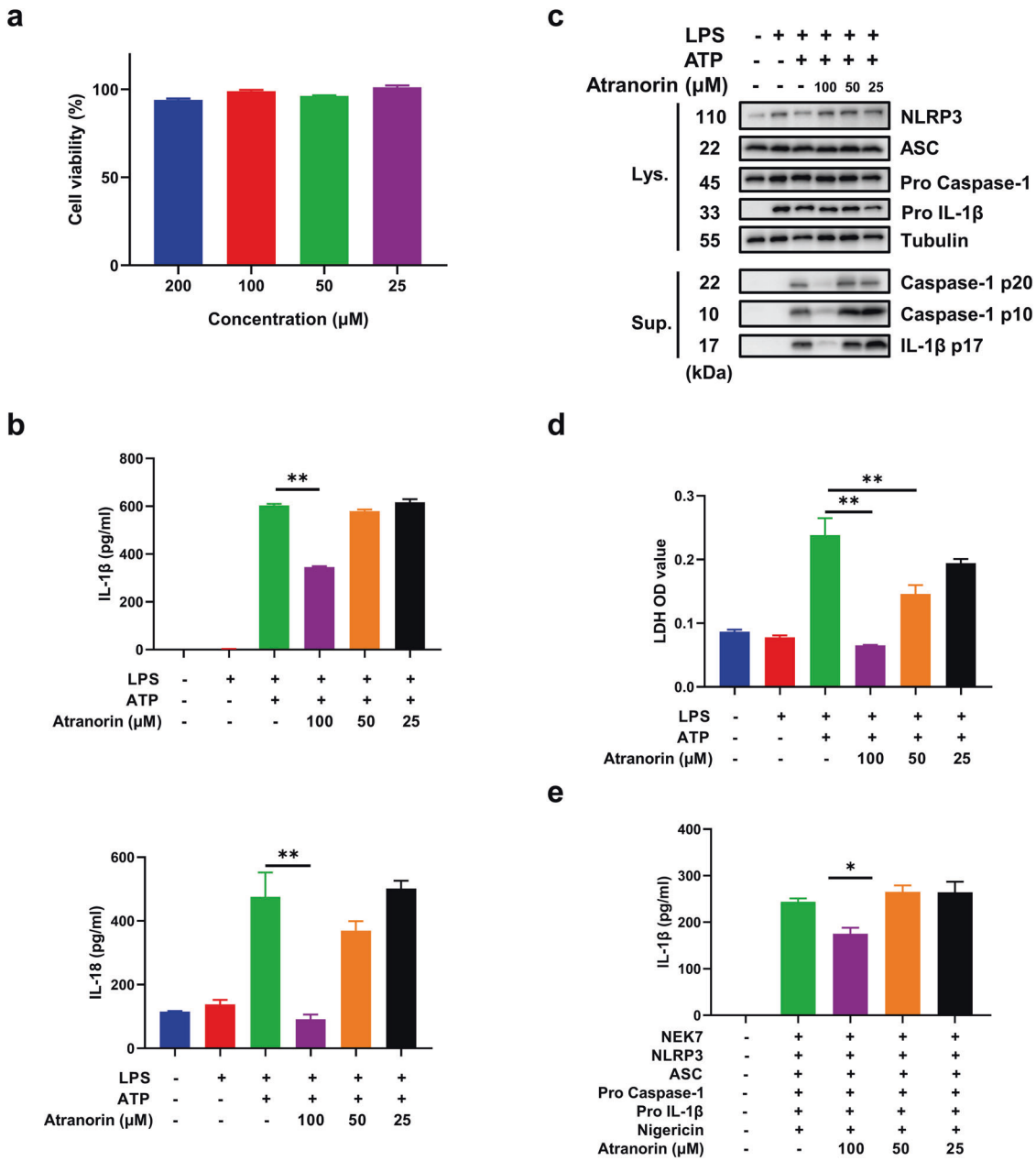

Fig. 2 Atranorin inhibits the activation of NLRP3 inflammasome in BMDC and NLRP3 inflammasome-reconstituted HEK293T cells. a The cytotoxicity of Atranorin on BMDC was detected by LDH kit. **b**–**d** BMDC were primed with LPS and then stimulated with ATP in the presence or absence of different doses of Atranorin. IL-1β and IL-18 levels in culture supernatants (**b**) were measured by ELISA. The protein levels of NLRP3, ASC, Pro Caspase-1 and Pro IL-1β in cell lysates and cleaved Caspase-1 and cleaved IL-1β in resin concentrated supernatants (**c**) were detected by Western blot. The LDH level in cell culture supernatants (**d**) was measured by LDH kit. **e** NLRP3 inflammasome components were transfected into HEK293T cells followed by Nigericin stimulation. IL-1β level in culture supernatants of NLRP3 inflammasome-reconstituted HEK293T cells was measured by ELISA. Data were shown as mean ± SEM from triplicate measurements. $^{*}P < 0.05$, $^{**}P < 0.01$ compared as indicated.

formation of ASC oligomer induced by ATP or Nigericin in BMDM (Fig. 3a). Meanwhile, Atranorin inhibited ASC speck formation, indicated by immunofluorescence assay (Fig. 3b). We speculated that Atranorin might directly bind to ASC and therefore inhibiting ASC oligomerization. Cellular thermal shift assay (CETSA) and drug affinity responsive target stability (DARTS) assay are well-established techniques for determining drug-target interactions [24, 25]. In CETSA assay, pre-incubation of Atranorin (100 μM) with BMDM increased the thermostability of ASC protein and retarded the heat-degradation effect on ASC (Fig. 3c). In DARTS assay, pre-incubation Atranorin with cell lysates of BMDM attenuated pronase induced proteolysis of ASC protein (Fig. 3d). Combing the results of CETSA and DARTS, we identified that Atranorin could bind to ASC protein directly. We then determined whether Atranorin inhibits NLRP3 inflammasome through binding to ASC. NLRP1B inflammasome could be activated independent of ASC since NLRP1B processes caspase activation and recruitment domains (CARDs) and can directly interact with Pro Caspase-1 to induce pyroptosis [26]. We used Val-BoroPro (VbP, also known as Talabostat), a newly defined ligand of NLRP1B [27] to activate NLRP1B inflammasome. In RAW264.7 macrophages, which do not express ASC [28],

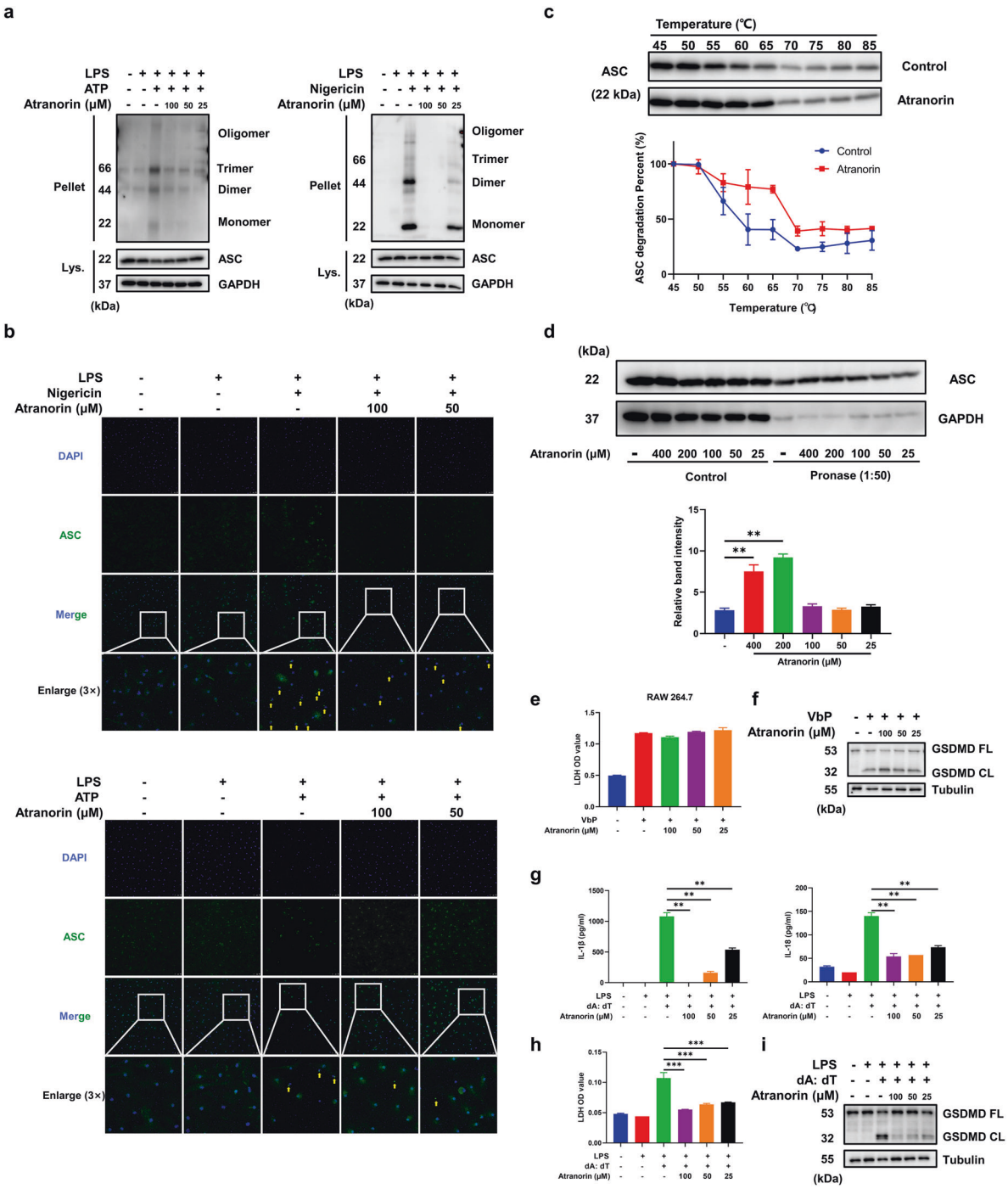

Fig. 3 Atranorin inhibits the assembly of NLRP3 inflammasome complex through binding to ASC. a, **b** BMDM were primed with LPS and then stimulated with ATP/Nigericin in the presence or absence of different doses of Atranorin. ASC levels in cell lysates and cross-linked cytosolic pellets (**a**) were detected by Western blot. BMDM were stained with FITC-conjugated ASC antibody and DAPI. ASC speck formation (**b**) was observed by immunofluorescence, indicated by the yellow arrows (scale = 50 μm). **c** The thermal stability of ASC protein in BMDM treated with or without Atranorin (100 μM) was measured by CETSA. **d** DARTS assay was performed with pronase (1:50) in the presence or absence of different doses of Atranorin. ASC protein level in lysates was analyzed by Western blot. The relative band intensity was calculated by comparing the pronase digested band with the control band after normalization with GAPDH. **e**, **f** RAW264.7 cells were stimulated with Val-BoroPro in the presence or absence of different doses of Atranorin. LDH level in culture supernatants (**e**) was measured by LDH kit. GSDMD full length and cleaved GSDMD in cell lysates (**f**) were measured by Western blot. **g**–**i** BMDM were primed with LPS and then transfected with Poly (dA: dT) in the presence or absence of different doses of Atranorin. IL-1β and IL-18 levels in culture supernatants (**g**) were measured by ELISA. LDH level in culture supernatants (**h**) was measured by LDH kit. GSDMD full length and cleaved GSDMD in cell lysates (**i**) were measured by Western blot. Data were shown as mean ± SEM from triplicate measurements. $^{*}P < 0.05$, $^{**}P < 0.01$ compared as indicated.

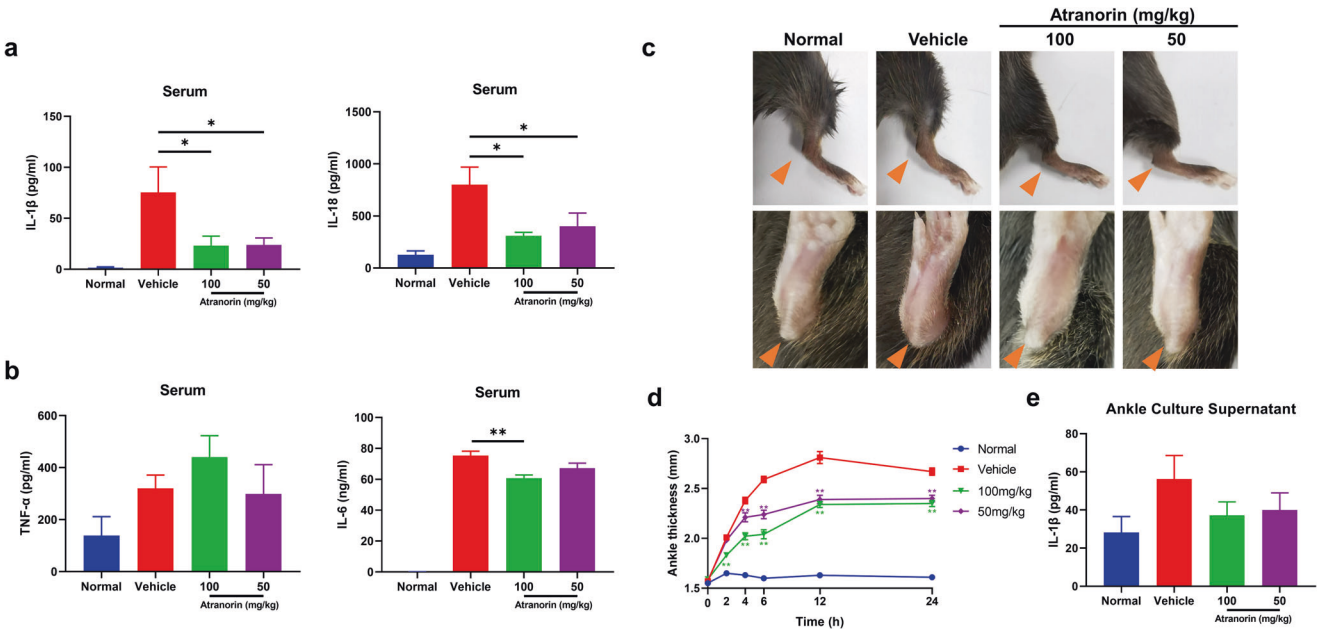

Fig. 4 Atranorin inhibits NLRP3 inflammation activation in LPS induced mice acute inflammation and MSU crystal induced mice gouty arthritis. a, **b** C57BL/6 mice were treated with or without different doses of Atranorin (i.g.) for 1 h and then challenged with LPS (i.p.) for 2 h ($n = 5$). Serum IL-1β and IL-18 levels (**a**) and serum TNF-α and IL-6 levels (**b**) were measured by ELISA. **c**–**e** C57BL/6 mice were pretreated with or without different doses of Atranorin (i.g.) for 1 h and then injected intra-articularly with MSU crystal ($n = 5$). Ankle swelling was shot at the end point (**c**) and was also measured at different time points. The orange arrow indicates the swelling of ankle joints (**d**). IL-1β level in ankle explant culture supernatant (**e**) was measured by ELISA. These results are representative of three independent experiments. Data were shown as mean ± SEM. $^*P < 0.05$, $^{**}P < 0.01$ compared with Vehicle group or as indicated.

Atranorin failed to inhibit LDH release (Fig. 3e) and GSDMD cleavage (Fig. 3f). AIM2 inflammasome shares the same assembly and activation process as NLRP3 inflammasome where ASC acts as the adapter molecule [29]. Atranorin suppressed AIM2 inflammasome activation in BMDM, indicated by the reduced IL-1β and IL-18 secretion (Fig. 3g), LDH release (Fig. 3h) and GSDMD cleavage (Fig. 3i). All these results suggest that Atranorin inhibits NLRP3 inflammasome assembly through binding to ASC.

Atranorin inhibits NLRP3 inflammation activation in LPS induced mice acute inflammation and MSU crystal induced mice gouty arthritis

To examine the therapeutic potential of Atranorin in vivo, we evaluated the effect of Atranorin in LPS induced mice acute inflammation model and MSU induced mice gouty arthritis model, which are the two most common used models for in vivo confirmation of NLRP3 inflammasome inhibition [19, 30–34]. LPS induced mice acute inflammation model is a well-characterized model of NLRP3 inflammasome-driven inflammation since the production of IL-1β was shown to be NLRP3 dependent [2]. We found that Atranorin treatment significantly decreased serum IL-1β and IL-18 levels (Fig. 4a). However, Atranorin did not significantly alter serum TNF-α level and showed milder inhibitory effect on serum IL-6 level, whose production is NLRP3 independent (Fig. 4b). Gouty arthritis is characterized by joint MSU crystal deposition. MSU is among the activator of NLRP3 inflammasome and gouty arthritis is regarded to be mediated by NLRP3 inflammasome [35]. Atranorin effectively ameliorated ankle joints swelling (Fig. 4c, d) in MSU crystal induced gouty arthritis mice. Meanwhile, Atranorin inhibited IL-1β secretion (with tendency) in the ankle joints explant culture supernatants (Fig. 4e). All the above data not only confirmed the in vivo activity of Atranorin on NLRP3 inhibition but also indicated the potential therapeutic application of Atranorin.

Atranorin alleviates DSS induced mice ulcerative colitis

Ulcerative colitis (UC) is a chronic and relapsing inflammatory disease characterized by epithelial barrier dysfunction and intestinal inflammation [36]. Although the etiology of UC has not been fully illustrated, NLRP3 inflammasome activation is recognized to mediate the pathogenesis of UC [37]. DSS induced colitis animal model could highly mimic human UC [38]. Also, DSS was reported to directly stimulate NLRP3 inflammasome activation and mature IL-1β release [39]. Therefore, DSS induced colitis was chosen in our study to further verify the pharmacological effect of Atranorin in NLRP3 inflammasome-driven diseases (Fig. 5a). Atranorin dose-dependently reduced weight loss, fecal bleeding and improved stool consistency as well as the DAI score during the UC progression (Fig. 5b). Consistently, the colon shortening was restored (Fig. 5c, d). Splenomegaly is associated with inflammation severity. Atranorin also decreased spleen index in DSS treated mice (Fig. 5e). We further evaluated the severity of colonic inflammation by histopathological analysis. DSS-treated mice exhibited obvious mucosal ulceration, crypt loss, goblet cells and epithelial damage, and immune cell infiltration in colon tissue. Atranorin could reverse these manifestations (Fig. 5f) and increase histology score (Fig. 5g). Epithelial barrier destruction is among the main characters of UC. We used In Vivo Imaging System (IVIS) technic to assess the intestinal permeability. FITC-dextran is nonmetabolizable macromolecule that mainly excreted through the intestinal tract and urethra. Once intestinal injury occurred, intestinal retention and blood penetration of FITC-CM-dextran would increase. Atranorin treatment lowered the absorption of FITC fluorescence both at abdomen (Fig. 5h) and in serum (Fig. 5i). In accordance, Atranorin recovered tight junction protein E-cadherin level in colon homogenates of UC mice (Fig. 5j). All these results indicate that Atranorin is able to alleviate DSS-induced mice UC.

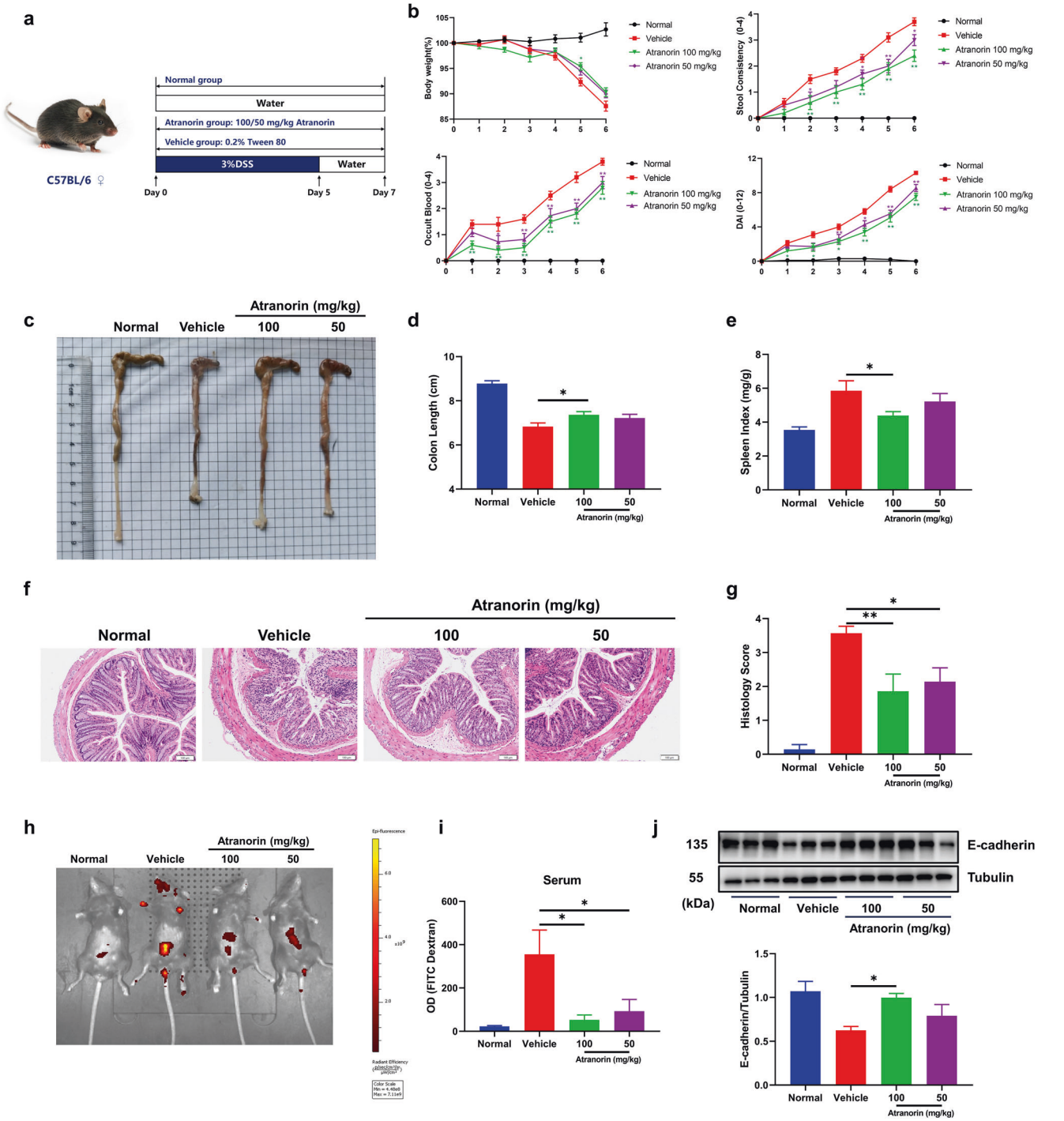

Fig. 5 Atranorin alleviates DSS induced mice ulcerative colitis. a The experiment design of DSS induced UC. C57BL/6 mice were treated with 3% DSS for 5 d and then sterile water for additional 2 d ($n = 10$). Atranorin was administered by oral daily. **b** Body weight, stool consistency, occult blood and disease activity index (DAI) were evaluated daily. **c** Typical appearances of colon. **d** The statistical analysis of colon length. **e** Spleen index was calculated as spleen weight/body weight (mg/g). **f** Typical microscopic pictures of H&E-stained colons (scale = 100 μm). **g** The statistical analysis of histological scores ($n = 7$). **h**, **i** FITC-dextran (600 mg/kg) was administered by oral gavage at d 7. Intestinal permeability was detected both by IVIS Spectrum (**h**) and by serum FITC-dextran fluorescence intensity (**i**). **j** The expression of tight junction protein E-cadherin in colon homogenates was detected by Western blot and quantified by normalization with Tubulin. These results are representative of three independent experiments. Data were shown as mean ± SEM. *$P < 0.05$, **$P < 0.01$ compared with Vehicle group or as indicated.

Atranorin inhibits NLRP3 inflammasome activation in DSS induced mice ulcerative colitis

We then evaluated whether Atranorin could inhibit NLRP3 inflammasome activation in UC mice. Firstly, we detected the protein levels of NLRP3 inflammasome complex and effector molecules in colon homogenates. In DSS treated group, the levels of NLRP3, Pro Caspase-1, Pro IL-1β, cleaved Caspase-1 p20/p10 and IL-1β p17 increased, indicating the activation of

NLRP3 inflammasome in colon. Atranorin administration did not influence the protein levels of NLRP3, Pro Caspase-1 and Pro IL-1β, but reduced the cleaved Caspase-1 p20/p10 and IL-1β p17 (with tendency) levels (Fig. 6a), suggesting that Atranorin inhibits NLRP3 inflammasome activation (Signal 2) without interfering the expression of NLRP3 inflammasome components (Signal 1) in colon. At the same time, the activation form of pyroptosis executor GSDMD in colon homogenates was decreased (Fig. 6a). In consist, Atranorin treatment lowered the levels of IL-1β and IL-18 in serum (Fig. 6b), colon explant culture supernatants (Fig. 6c) and colon homogenates (Fig. 6d). Infiltration of macrophages and dendritic cells is not only the manifestation but also the promotor of UC [40, 41]. To observe the activation of NLRP3 inflammasome in colon macrophages and dendritic cells, we stained macrophages and dendritic cells with F4/80 and CD11c, respectively to indicate infiltration and stained caspase-1 p20 subunit to indicate NLRP3 inflammasome activation. Atranorin not only significantly reduced the infiltration of macrophages (Fig. 6e) and dendritic cells (Fig. 6f) in colon but also inhibited the activation of NLRP3 inflammasome. Hence, we concluded that Atranorin could inhibit NLRP3 inflammasome activation in DSS induced UC mice.

DISCUSSION

In this article, we identify Atranorin as a potential NLRP3 inflammation inhibitor. Atranorin suppresses NLRP3 inflammation activation through binding to ASC and inhibiting ASC oligomerization without influencing the priming stage. What's more, Atranorin effectively protects NLRP3 inflammasome mediated diseases including acute inflammation, gouty arthritis and UC (Fig. 7).

Atranorin is the secondary metabolite metabolites of lichen families with multidirectional biological activities [42]. Although the potential anti-inflammatory activity of Atranorin has been identified, the in-depth mechanism study is lacking. In this study, we first confirmed that Atranorin inhibits multiply stimulus induced NLRP3 inflammasome activation in BMDM and BMDC by applying Atranorin after the LPS priming stage and before the activation stage, indicated by reduced Caspase-1 process, cytokines secretion and pyroptosis. The reduced IL-1β level in NLRP3 inflammasome-reconstituted HEK293T cells also supports this conclusion, Interestingly, when applied at the priming stage and wash away before the activation stage, Atranorin did not influence the transcript of NLRP3 component or LDH release, suggesting that Atranorin acts at the activation stage rather than the priming stage of NLRP3 activation, which would avoid side effects caused by NF-κB inhibition [8].

ASC is the central component of NLRP3 inflammasome complex that consists of the N-terminal pyrin domain (PYD) and the C-terminal CARD. ASC would aggregate into filaments through PYD-PYD interactions and condense as speck via CARD-CARD interactions to promote NLRP3 inflammasome activation [43]. In our study, we found that Atranorin could inhibit ASC oligomerization. The results of CETSA and DARTS verified that Atranorin directly binds to ASC. To verify whether Atranorin inhibits NLRP3 inflammasome through binding to ASC, we tested the influence of Atranorin on the activation of other inflammasome that dependent or independent of ASC. NLRP1B inflammasome could be activated independent of ASC since NLRP1B processes CARDs and can directly interact with Pro Caspase-1 [26, 44]. Whereas, when ASC is absent, Pro Caspase-1 does not efficiently process itself and IL-1β but only cleaves and activates GSDMD to induce pyroptosis [45]. We found Atranorin failed to inhibit LDH release and GSDMD cleavage induced by NLRP1B activator Val-BoroPro in RAW264.7 macrophages that lacking ASC [28]. In contrast, Atranorin could inhibit AIM2 inflammasome activation in BMDM, where ASC serves as the adapter molecular [29]. These results confirmed that Atranorin inhibits NLRP3 inflammasome activation through binding to ASC. It is applicable to define the binding pattern of Atranorin toward ASC protein in our future study since human and mouse ASC-PYD filaments have been successfully reconstituted in vitro and their structures have already been solved [46, 47].

Considering the role of ASC in NLRP3 inflammasome, targeting ASC with small molecular compound [48] or monoclonal antibody [49, 50] is proposed applicable for directly inhibiting NLRP3 inflammasome as well as for treating NLRP3 related diseases. ASC is also the adapter molecular of other inflammasome such as AIM2, PYRIN and NLRP6 inflammasome. Therefore, Atranorin might be feasible to treat inflammatory diseases driven by other inflammasomes whose activation is ASC dependent. Moreover, recent studies showed that some specific inflammatory diseases are driven by several kinds of inflammasomes concurrently. Thus, through targeting ASC, Atranorin might have therapeutic effects toward complicated diseases that associated with more than one inflammasome, such as experimental autoimmune encephalomyelitis (EAE) [51–53] and systemic lupus erythematosus (SLE) [54].

In our study, we first evaluated whether Atranorin could inhibit NLRP3 inflammasome activation in vivo by introducing LPS induced acute inflammation and MSU crystal induced gouty arthritis models. The doses of Atranorin used in our experiments (100 mg/kg and 50 mg/kg) were selected according to the published articles as well as the results of subchronic toxicity study and acute toxicity study [17]. We showed that Atranorin inhibited IL-1β and IL-18 production in LPS induced acute inflammation mice and protected against MSU crystal induced mice gouty arthritis, confirming the therapeutic potential of Atranorin toward NLRP3 inflammasome related diseases.

We then studied the pharmacological effect of Atranorin on DSS induced mice UC. UC is a chronic inflammatory disorder that occurs in colonic mucosa. NLRP3 inflammasome and its signaling molecules are recognized to mediate the pathogenesis of UC [4]. We discovered Atranorin could alleviate DSS induced mice UC and prevent activation of NLRP3 inflammasome in colon macrophages and dendritic cells. IL-1β could induce the expression of adhesion molecules and chemokines, thus promoting the infiltration of inflammatory and immunocompetent cells from the circulation into lesional tissues [55]. This property of IL-1β might explain the phenomenon that Atranorin prevented the infiltration of macrophages and dendritic cells in colon. We also observed the protective effect of Atranorin on the decreased intestinal permeability. This might be owing to the results of NLRP3 inflammasome inhibition, since IL-1β could increases intestinal tight junction permeability [56–58]. Intestinal microbiota dysbiosis is involved in UC progress [59]. The gut microbiota was identified to induce the expression and activation of inflammasome proteins, which contribute to both homeostasis and disease in UC [60]. Atranorin possesses significant antibacterial activity [16, 61, 62]. Whether Atranorin could ameliorate UC through regulating intestinal microbiota is an interesting topic that remains to study.

All together, we identify that lichen secondary metabolite Atranorin inhibits NLRP3 inflammasome activation through binding to ASC and alleviates NLRP3 inflammasome-driven disease models including LPS induced acute inflammation, MSU crystal induced gouty arthritis and DSS induced colitis. Our study not only uncover the potential pharmacological application of Atranorin but also contribute to the development of nature product derived NLRP3 inhibitors.

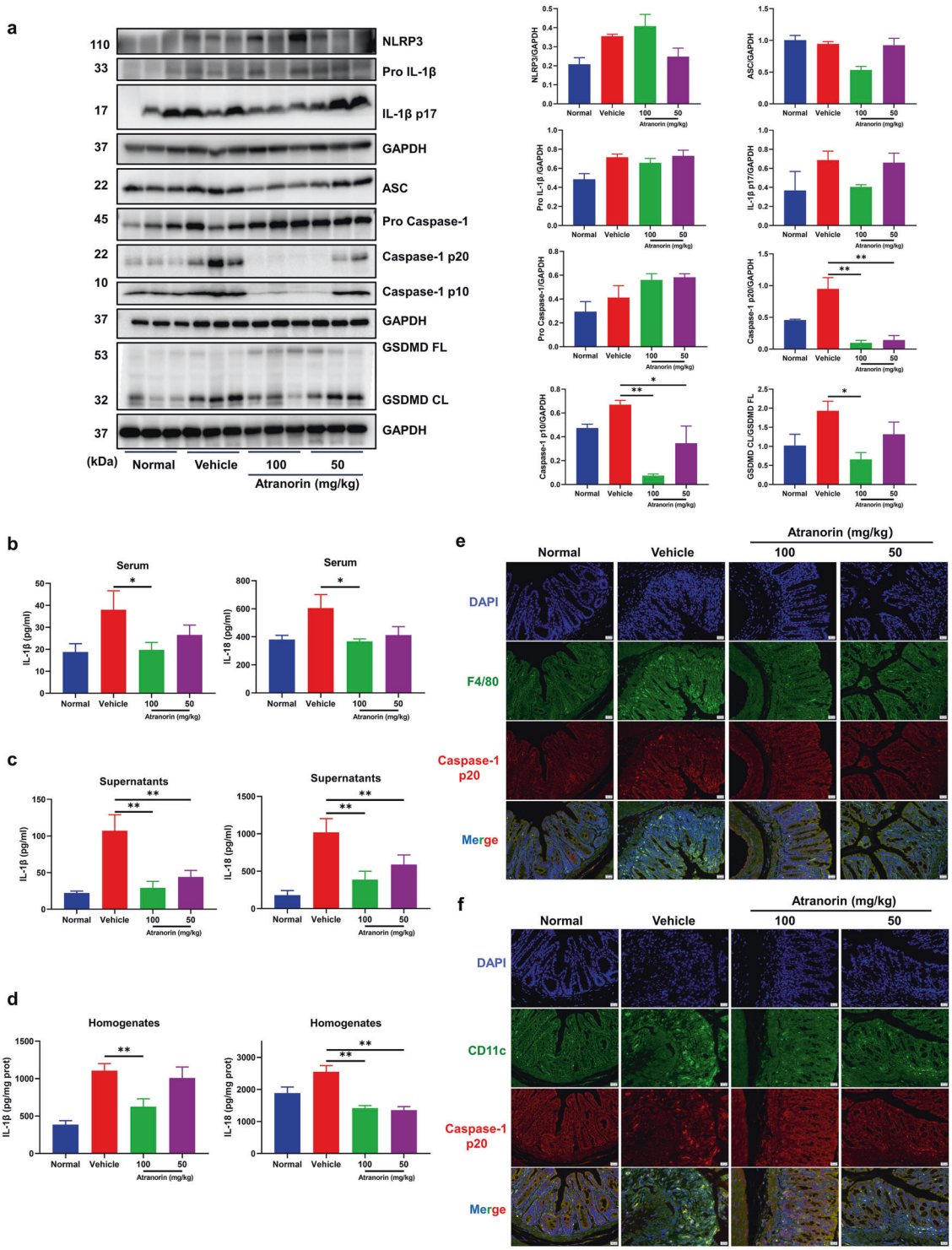

Fig. 6 Atranorin inhibits NLRP3 inflammasome activation in DSS induced mice ulcerative colitis. a The protein levels of NLRP3, Pro IL-1β, cleaved IL-1β, ASC, Pro Caspase-1, cleaved Caspase-1, GSDMD and cleaved GSDMD (N-terminal fragment) in colon homogenates were detected by Western blot and quantified by normalization with GAPDH or GSDMD FL. **b**–**d** IL-1β and IL-18 levels in serum (**b**), colon explant culture supernatants (**c**), and colon homogenates (**d**) were measured by ELISA. **e**, **f** Colon infiltration of macrophages (stained with F4/80) and dendritic cells (stained with CD11c) and the activation of NLRP3 inflammasome (stained with Caspase-1 p20) in colon macrophages (**e**) and dendritic cells (**f**) were detected by immunofluorescence. These results are representative of three independent experiments. Data were shown as mean ± SEM. $^{*}P < 0.05$, $^{**}P < 0.01$ compared with Vehicle group or as indicated.

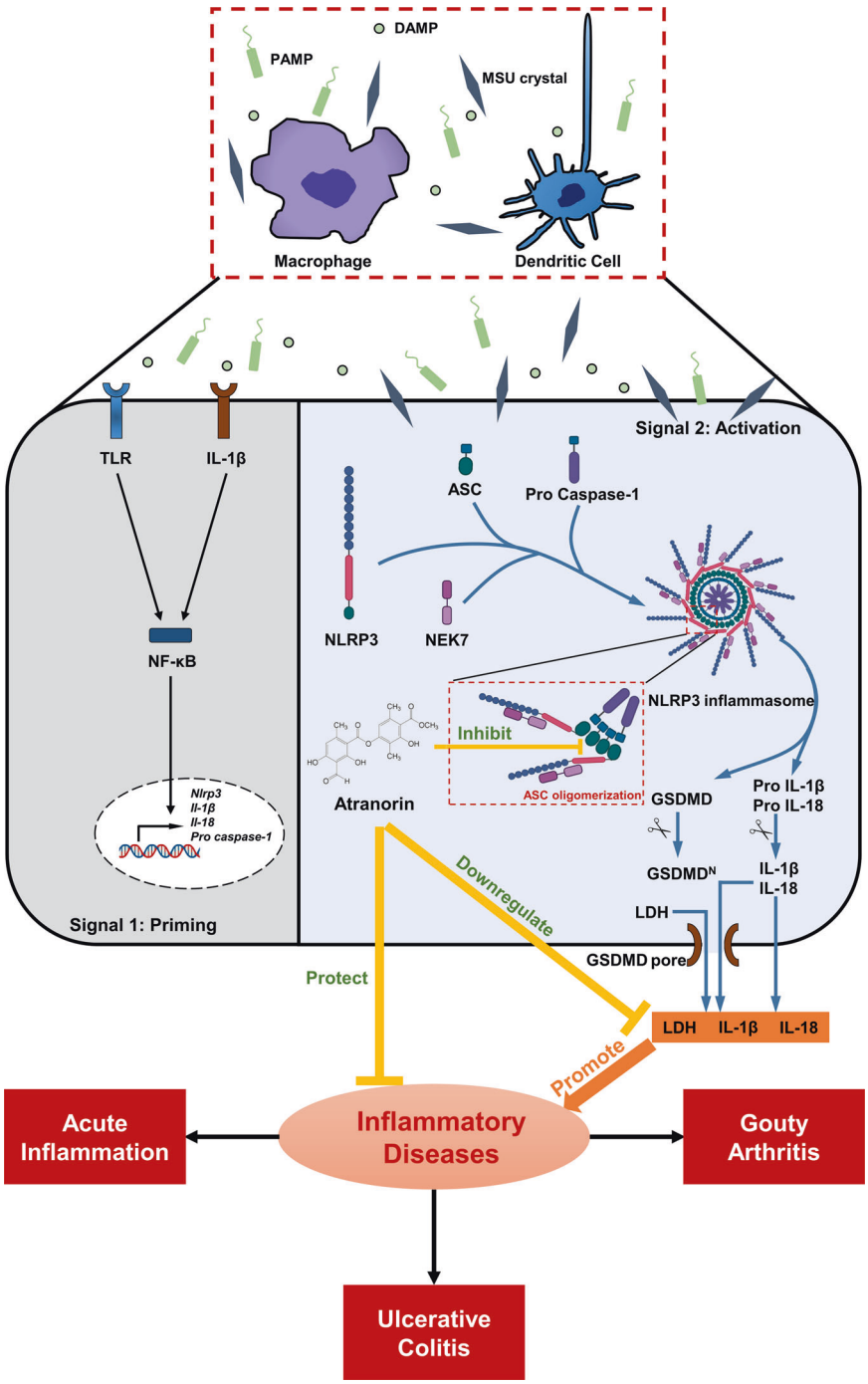

Fig. 7 Atranorin inhibits NLRP3 inflammasome activation by targeting ASC and protects against NLRP3 inflammasome-driven diseases. Atranorin suppresses NLRP3 inflammation activation induced cytokines release and pyroptosis through binding to ASC and inhibiting ASC oligomerization. Atranorin also attenuates NLRP3 inflammasome-driven disease models including LPS induced acute inflammation, MSU crystal induced gouty arthritis and DSS induced mouse colitis.

ACKNOWLEDGEMENTS

This work was supported by the grants of National Natural Science Foundation of China (NSFC) (No. 82173823). We thank Professor Wei-min Zhao for providing Atranorin, Bing Wu, Fang Bai, Meng-meng Xu and Hao Li for their kind assistance to this study.

AUTHOR CONTRIBUTIONS

HYW: Conceptualization, Investigation, Methodology, Formal analysis, Writing - original draft. XL: Investigation, Validation, Formal analysis. GGH: Investigation, Validation. RZ: Investigation, Formal analysis. SYL: Investigation. JR: Investigation. KRZ: Investigation. CLF: Resources, Data curation. YWW: Conceptualization, Funding acquisition, Supervision, Writing - review & editing. WT: Conceptualization, Funding acquisition, Project administration, Resources, Supervision, Resources, Writing - review & editing.

ADDITIONAL INFORMATION

Supplementary information The online version contains supplementary material available at https://doi.org/10.1038/s41401-023-01054-1.

Competing interests: The authors declare no competing interests.

REFERENCES

1. Swanson KV, Deng M, Ting JP. The NLRP3 inflammasome: molecular activation and regulation to therapeutics. Nat Rev Immunol. 2019;19:477–89.
2. He Y, Franchi L, Nunez G. TLR agonists stimulate Nlrp3-dependent IL-1beta production independently of the purinergic P2X7 receptor in dendritic cells and in vivo. J Immunol. 2013;190:334–9.
3. Szekanecz Z, Szamosi S, Kovacs GE, Kocsis E, Benko S. The NLRP3 inflammasome - interleukin 1 pathway as a therapeutic target in gout. Arch Biochem Biophys. 2019;670:82–93.
4. Mao L, Kitani A, Strober W, Fuss IJ. The role of NLRP3 and IL-1beta in the pathogenesis of inflammatory bowel disease. Front Immunol. 2018;9:2566.
5. Mangan MSJ, Olhava EJ, Roush WR, Seidel HM, Glick GD, Latz E. Targeting the NLRP3 inflammasome in inflammatory diseases. Nat Rev Drug Discov. 2018;17:588–606.
6. Kinra M, Nampoothiri M, Arora D, Mudgal J. Reviewing the importance of TLR-NLRP3-pyroptosis pathway and mechanism of experimental NLRP3 inflammasome inhibitors. Scand J Immunol. 2022;95:e13124.
7. Blevins HM, Xu Y, Biby S, Zhang S. The NLRP3 inflammasome pathway: a review of mechanisms and inhibitors for the treatment of inflammatory diseases. Front Aging Neurosci. 2022;14:879021.
8. Greten FR, Arkan MC, Bollrath J, Hsu LC, Goode J, Miething C, et al. NF-kappaB is a negative regulator of IL-1beta secretion as revealed by genetic and pharmacological inhibition of IKKbeta. Cell. 2007;130:918–31.
9. Hayden MS, Ghosh S. NF-kappaB in immunobiology. Cell Res. 2011;21:223–44.
10. Su CC, Wang SC, Chen IC, Chiu FY, Liu PL, Huang CH, et al. Zerumbone suppresses the LPS-induced inflammatory response and represses activation of the NLRP3 inflammasome in macrophages. Front Pharmacol. 2021;12:652860.
11. Kuemmerle-Deschner JB, Hachulla E, Cartwright R, Hawkins PN, Tran TA, Bader-Meunier B, et al. Two-year results from an open-label, multicentre, phase III study evaluating the safety and efficacy of canakinumab in patients with cryopyrin-associated periodic syndrome across different severity phenotypes. Ann Rheum Dis. 2011;70:2095–102.
12. Dinarello CA, van der Meer JW. Treating inflammation by blocking interleukin-1 in humans. Semin Immunol. 2013;25:469–84.
13. Suzuki MT, Parrot D, Berg G, Grube M, Tomasi S. Lichens as natural sources of biotechnologically relevant bacteria. Appl Microbiol Biotechnol. 2016;100:583–95.
14. Mendili M, Khadhri A, Mediouni-Ben Jemaa J, Andolfi A, Tufano I, Aschi-Smiti S, et al. Anti-inflammatory potential of compounds isolated from tunisian lichens species. Chem Biodivers. 2022;19:e202200134.
15. Kumar KC, Muller K. Lichen metabolites. 1. Inhibitory action against leukotriene B4 biosynthesis by a non-redox mechanism. J Nat Prod. 1999;62:817–20.
16. Bugni TS, Andjelic CD, Pole AR, Rai P, Ireland CM, Barrows LR. Biologically active components of a Papua New Guinea analgesic and anti-inflammatory lichen preparation. Fitoterapia. 2009;80:270–3.
17. de Melo MGD, Araujo AAD, Serafini MR, Carvalho LF, Bezerra MS, Ramos CS, et al. Anti-inflammatory and toxicity studies of atranorin extracted from Cladina kalbii Ahti in rodents. Braz J Pharm Sci. 2011;47:861–72.
18. Shi H, Murray A, Beutler B. Reconstruction of the mouse inflammasome system in HEK293T cells. Bio Protoc. 2016;6:e1986.
19. Coll RC, Robertson AA, Chae JJ, Higgins SC, Munoz-Planillo R, Inserra MC, et al. A small-molecule inhibitor of the NLRP3 inflammasome for the treatment of inflammatory diseases. Nat Med. 2015;21:248–55.
20. Jafari R, Almqvist H, Axelsson H, Ignatushchenko M, Lundback T, Nordlund P, et al. The cellular thermal shift assay for evaluating drug target interactions in cells. Nat Protoc. 2014;9:2100–22.
21. Pai MY, Lomenick B, Hwang H, Schiestl R, McBride W, Loo JA, et al. Drug affinity responsive target stability (DARTS) for small-molecule target identification. Methods Mol Biol. 2015;1263:287–98.
22. Zhong Y, Kinio A, Saleh M. Functions of NOD-like receptors in human diseases. Front Immunol. 2013;4:333.
23. Hoss F, Rodriguez-Alcazar JF, Latz E. Assembly and regulation of ASC specks. Cell Mol Life Sci. 2017;74:1211–29.
24. Martinez Molina D, Jafari R, Ignatushchenko M, Seki T, Larsson EA, Dan C, et al. Monitoring drug target engagement in cells and tissues using the cellular thermal shift assay. Science. 2013;341:84–87.
25. Lomenick B, Hao R, Jonai N, Chin RM, Aghajan M, Warburton S, et al. Target identification using drug affinity responsive target stability (DARTS). Proc Natl Acad Sci USA. 2009;106:21984–9.
26. Poyet JL, Srinivasula SM, Tnani M, Razmara M, Fernandes-Alnemri T, Alnemri ES. Identification of Ipaf, a human caspase-1-activating protein related to Apaf-1. J Biol Chem. 2001;276:28309–13.
27. Okondo MC, Rao SD, Taabazuing CY, Chui AJ, Poplawski SE, Johnson DC, et al. Inhibition of Dpp8/9 activates the Nlrp1b inflammasome. Cell Chem Biol. 2018;25:262–7.e265.
28. Pelegrin P, Barroso-Gutierrez C, Surprenant A. P2X7 receptor differentially couples to distinct release pathways for IL-1beta in mouse macrophage. J Immunol. 2008;180:7147–57.
29. Lugrin J, Martinon F. The AIM2 inflammasome: sensor of pathogens and cellular perturbations. Immunol Rev. 2018;281:99–114.
30. Chen Y, He H, Lin B, Chen Y, Deng X, Jiang W, et al. RRx-001 ameliorates inflammatory diseases by acting as a potent covalent NLRP3 inhibitor. Cell Mol Immunol. 2021;18:1425–36.
31. Xu G, Fu S, Zhan X, Wang Z, Zhang P, Shi W, et al. Echinatin effectively protects against NLRP3 inflammasome-driven diseases by targeting HSP90. JCI Insight. 2021;6:e134601.
32. Marchetti C, Swartzwelter B, Gamboni F, Neff CP, Richter K, Azam T, et al. OLT1177, a beta-sulfonyl nitrile compound, safe in humans, inhibits the NLRP3 inflammasome and reverses the metabolic cost of inflammation. Proc Natl Acad Sci USA. 2018;115:E1530–E1539.
33. Wu J, Luo Y, Jiang Q, Li S, Huang W, Xiang L, et al. Coptisine from Coptis chinensis blocks NLRP3 inflammasome activation by inhibiting caspase-1. Pharmacol Res. 2019;147:104348.
34. Xu X, Li J, Long X, Tao S, Yu X, Ruan X, et al. C646 protects against DSS-induced colitis model by targeting NLRP3 inflammasome. Front Pharmacol. 2021;12:707610.
35. Martinon F, Pétrilli V, Mayor A, Tardivel A, Tschopp J. Gout-associated uric acid crystals activate the NALP3 inflammasome. Nature. 2006;440:237–41.
36. Ungaro R, Mehandru S, Allen PB, Peyrin-Biroulet L, Colombel JF. Ulcerative colitis. Lancet. 2017;389:1756–70.
37. Zhen Y, Zhang H. NLRP3 inflammasome and inflammatory bowel disease. Front Immunol. 2019;10:276.
38. Mizoguchi A. Animal models of inflammatory bowel disease. Prog Mol Biol Transl Sci. 2012;105:263–320.
39. Bauer C, Duewell P, Mayer C, Lehr HA, Fitzgerald KA, Dauer M, et al. Colitis induced in mice with dextran sulfate sodium (DSS) is mediated by the NLRP3 inflammasome. Gut. 2010;59:1192–9.
40. Watanabe S, Yamakawa M, Hiroaki T, Kawata S, Kimura O. Correlation of dendritic cell infiltration with active crypt inflammation in ulcerative colitis. Clin Immunol. 2007;122:288–97.
41. Yan YX, Shao MJ, Qi Q, Xu YS, Yang XQ, Zhu FH, et al. Artemisinin analogue SM934 ameliorates DSS-induced mouse ulcerative colitis via suppressing neutrophils and macrophages. Acta Pharmacol Sin. 2018;39:1633–44.
42. Studzinska-Sroka E, Galanty A, Bylka W. Atranorin - an interesting lichen secondary metabolite. Mini Rev Med Chem. 2017;17:1633–45.
43. Dick MS, Sborgi L, Ruhl S, Hiller S, Broz P. ASC filament formation serves as a signal amplification mechanism for inflammasomes. Nat Commun. 2016;7:11929.
44. Van Opdenbosch N, Gurung P, Vande Walle L, Fossoul A, Kanneganti T-D, Lamkanfi M. Activation of the NLRP1b inflammasome independently of ASC-mediated caspase-1 autoproteolysis and speck formation. Nat Commun. 2014;5:3209.
45. Okondo MC, Johnson DC, Sridharan R, Go EB, Chui AJ, Wang MS, et al. DPP8 and DPP9 inhibition induces pro-caspase-1-dependent monocyte and macrophage pyroptosis. Nat Chem Biol. 2017;13:46–53.
46. Lu A, Magupalli VG, Ruan J, Yin Q, Atianand MK, Vos MR, et al. Unified polymerization mechanism for the assembly of ASC-dependent inflammasomes. Cell. 2014;156:1193–206.
47. Sborgi L, Ravotti F, Dandey VP, Dick MS, Mazur A, Reckel S, et al. Structure and assembly of the mouse ASC inflammasome by combined NMR spectroscopy and cryo-electron microscopy. Proc Natl Acad Sci USA. 2015;112:13237–42.
48. Lee HE, Yang G, Kim ND, Jeong S, Jung Y, Choi JY, et al. Targeting ASC in NLRP3 inflammasome by caffeic acid phenethyl ester: a novel strategy to treat acute gout. Sci Rep. 2016;6:38622.
49. Desu HL, Plastini M, Illiano P, Bramlett HM, Dietrich WD, de Rivero Vaccari JP, et al. IC100: a novel anti-ASC monoclonal antibody improves functional outcomes in an animal model of multiple sclerosis. J Neuroinflammation. 2020;17:143.
50. de Rivero Vaccari JP, Mim C, Hadad R, Cyr B, Stefansdottir TA, Keane RW. Mechanism of action of IC100, a humanized IgG4 monoclonal antibody targeting apoptosis-associated speck-like protein containing a caspase recruitment domain (ASC). Transl Res. 2023;251:27–40.
51. Shao S, Chen C, Shi G, Zhou Y, Wei Y, Fan N, et al. Therapeutic potential of the target on NLRP3 inflammasome in multiple sclerosis. Pharmacol Ther. 2021;227:107880.
52. Barclay WE, Aggarwal N, Deerhake ME, Inoue M, Nonaka T, Nozaki K, et al. The AIM2 inflammasome is activated in astrocytes during the late phase of EAE. JCI Insight. 2022;7:e155563.
53. Dumas A, Amiable N, de Rivero Vaccari JP, Chae JJ, Keane RW, Lacroix S, et al. The inflammasome pyrin contributes to pertussis toxin-induced IL-1beta synthesis,

neutrophil intravascular crawling and autoimmune encephalomyelitis. PLoS Pathog. 2014;10:e1004150.
54. Yang CA, Huang ST, Chiang BL. Sex-dependent differential activation of NLRP3 and AIM2 inflammasomes in SLE macrophages. Rheumatology. 2015;54:324–31.
55. Dinarello CA. Immunological and inflammatory functions of the interleukin-1 family. Annu Rev Immunol. 2009;27:519–50.
56. Rawat M, Nighot M, Al-Sadi R, Gupta Y, Viszwapriya D, Yochum G, et al. IL1B increases intestinal tight junction permeability by up-regulation of MIR200C-3p, which degrades occludin mRNA. Gastroenterology. 2020;159:1375–89.
57. Al-Sadi RM, Ma TY. IL-1beta causes an increase in intestinal epithelial tight junction permeability. J Immunol. 2007;178:4641–9.
58. Kaminsky LW, Al-Sadi R, Ma TY. IL-1beta and the intestinal epithelial tight junction barrier. Front Immunol. 2021;12:767456.
59. Ni J, Wu GD, Albenberg L, Tomov VT. Gut microbiota and IBD: causation or correlation? Nat Rev Gastroenterol Hepatol. 2017;14:573–84.
60. Watanabe D, Guo Y, Kamada N. Interaction between the inflammasome and commensal microorganisms in gastrointestinal health and disease. EMBO Mol Med. 2021;13:e13452.
61. Rankovic B, Misic M, Sukdolak S. The antimicrobial activity of substances derived from the lichens *Physcia aipolia*, *Umbilicaria polyphylla*, *Parmelia caperata* and *Hypogymnia physodes*. World J Microbiol Biotechnol. 2008;24:1239–42.
62. Kocovic A, Jeremic J, Bradic J, Sovrlic M, Tomovic J, Vasiljevic P, et al. Phytochemical analysis, antioxidant, antimicrobial, and cytotoxic activity of different extracts of *Xanthoparmelia stenophylla* Lichen from Stara Planina, Serbia. Plants. 2022;11:1624.